COMPARISON OF COHESIVE ZONE MODELS USED TO PREDICT DELAMINATION INITIATED FROM FREE-EDGES : VALIDATION AGAINST EXPERIMENTAL RESULTS

A. Uguen *[1], L. Zubillaga[2], A. Turon[3], N. Carrère[1]

[1] *Laboratoire Brestois de Mécanique et des Systèmes EA 4325, ENSTA Bretagne/UBO/ENIB, 2 rue François Verny, 29806 Brest cedex 9, France*

[2] *IK4-Ikerlan, P^o. J. M^a. Arizmendiarrieta 2, 20500 Arrasate-Mondragn, Gipuzkoa, Spain*

[3] *AMADE, Polytechnic School, University of Girona, Campus Montilivi s/n, 17071 Girona, Spain*

* *Corresponding Author: alexandre.uguen@ensta-bretagne.fr*

Keywords: Composites, Delamination, Cohesive zone model, Experimental validation, Modeling

Abstract

The objective of this paper is to predict the free-edge delamination of composite materials. For this purpose a comparison between different cohesive zone models is presented as well as the different parameters which influence the damage law. To compare these models an experimental campaign was performed on five different stacks orientations of T800/M21 carbon epoxy composite laminate. Two different cohesive zone models were selected for the comparison with the experimental data. A good correlation was found between the predictions and the results of the experimental campaign.

1. Introduction

Composite materials have been widely used in industries such as the aerospace, the naval and the automotive sectors due to their excellent mechanical properties, low density and ease of manufacture. Despite of these advantages, some damage mechanisms remain critical. One of those is delamination which is caused by the weak mechanical properties of the interface between plies. This delamination problem is represented by two phenomena, the crack initiation and the crack propagation. This first phenomenon is created by out-of-plane stresses mainly generated near the edges of composite laminates due to the mismatch in elastic properties between plies. Once delamination has started, if the available energy release rate of the interface is higher than the fracture energy toughness, delamination propagation occurs. Different models are used to predict propagation in accordance with fracture mechanics tests. On the contrary, only very few models are employed to validate delamination initiation, like the coupled criterion [1] or the cohesive zone models [2].

These cohesive zone models have been developed to predict both delamination crack initiation and propagation of composite materials and to obtain the best possible description of delamination. Damage of the composite laminate is introduced through a damage law which links the displacement jumps of the interface with the associated cohesive tractions.

The purpose of this paper is to compare the results obtained by different cohesive zone models with experimental results in order to determine the accuracy of such models. First, the experimental campaign performed with T800/M21 carbon epoxy composite materials used to compare the results will be introduced. Then the different cohesive zone models established for this study will be explained such as the numerous parameters that govern the cohesive law. Finally the results obtained will be discussed thanks to the experimental data in order to determine the most important parameters of cohesive zone models and to evaluate the accuracy of such models.

2. Experimental campaign

An experimental campaign has been carried out on T800/M21 carbon-epoxy composite laminates. The five different lay-ups which have been tested are the following ones : $[\pm 10_2]_s$, $[\pm 20]_s$, $[\pm 20_2]_s$, $[\pm 20_3]_s$ and $[\pm 30_2]_s$. These lay-ups have been chosen in order to study the influence of the ply thickness with $[\pm 20]_s$, $[\pm 20_2]_s$ and $[\pm 20_3]_s$ lay-ups and the influence of the layers orientation with $[\pm 10_2]_s$, $[\pm 20_2]_s$ and $[\pm 30_2]_s$ lay-ups. The material properties of T800/M21 used in this study can be found in Table 1.

Laminate properties					
$\mathbf{E_{11}}$ (GPa)	$\mathbf{E_{22}}$=$\mathbf{E_{33}}$ (GPa)	$\mathbf{G_{12}}$=$\mathbf{G_{13}}$ (GPa)	$\mathbf{G_{23}}$ (GPa)	$\boldsymbol{\nu_{12}}$=$\boldsymbol{\nu_{13}}$	$\boldsymbol{\nu_{23}}$
130	8	4	4	0.31	0.45
Interfacial properties					
$\mathbf{G_{Ic}}$ (J/m^2)	$\mathbf{G_{IIc}}$=$\mathbf{G_{IIIc}}$ (J/m^2)	$\boldsymbol{\sigma^0_{zz}}$ (MPa)	$\boldsymbol{\sigma^0_{xz}}$=$\boldsymbol{\sigma^0_{yz}}$ (MPa)		
240	740	46	75		

Table 1. Material properties of T800/M21 used for the modeling.

The specimens were tested on a universal testing machine under tensile load. Two different measuring techniques were used. On the one hand the digital image correlation (from GOM technology) was used to ensure accurate displacement measures. On the other hand acoustic emissions were used to monitor the damage progression thanks to two sensors from Physical Acoustic Corporation. Further details and more information about these tests can be found in [3].

3. Modeling

3.1. Cohesive Zone Model

The cohesive zone model presented in this work is the one proposed by Abaqus software [4] with 3D elements. This model assumes that all damage mechanisms occurring at the interface can be taken into account by three-dimensional cohesive elements. The constitutive behavior of this interface is modeled as a relation between tractions t and associated displacement jumps δ through a softening law, as illustrated in Figure 1. This law is composed of three distinct parts. First of all, cohesive elements are associated with an initial stiffness which can be linked to the matrix Young modulus and to the thickness of the interface (1). It must be small enough not to increase the composite stiffness and high enough to respect the material properties. Then

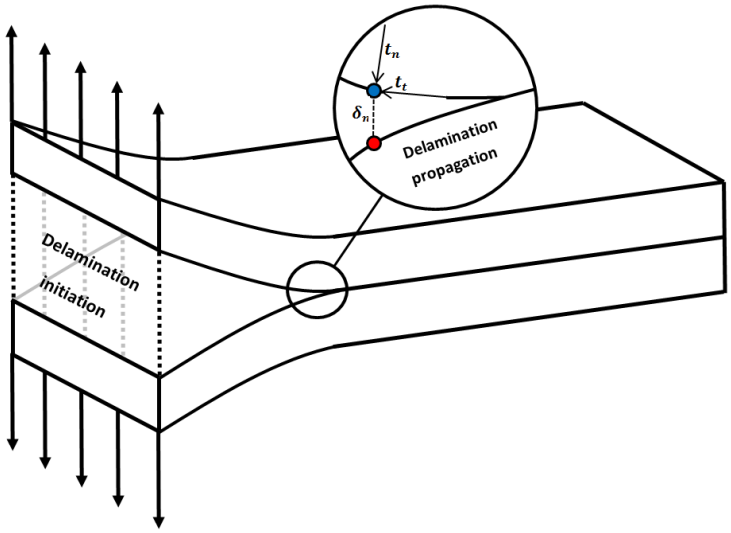

Figure 1. Cohesive tractions and displacement jumps at the interface of a DCB specimen.

the interlaminar stress increases until reaching a critical value (2). The damage initiates when the maximum nominal stress or the quadratic nominal stress criterion, both criteria, reaches the value of one. These criteria can be represented as :

$$max\left\{\frac{\langle\sigma_{zz}\rangle}{\sigma^0_{zz}}, \frac{\tau_{xz}}{\sigma^0_{xz}}, \frac{\tau_{yz}}{\sigma^0_{yz}}\right\} = 1 \qquad \text{and} \qquad \left\{\frac{\langle\sigma_{zz}\rangle}{\sigma^0_{zz}}\right\}^2 + \left\{\frac{\tau_{xz}}{\sigma^0_{xz}}\right\}^2 + \left\{\frac{\tau_{yz}}{\sigma^0_{yz}}\right\}^2 = 1 \tag{1}$$

where σ_{zz}, τ_{xz} and τ_{yz} are respectively the normal and the out-of-plane shear tractions. σ^0_{zz}, σ^0_{xz} and σ^0_{yz} are respectively the tensile out-of-plane strength and the out-of-plane shear strength in the plane xz and yz. The symbol $\langle\rangle$ represents the Macaulay brackets signifying that a pure compression state does not damage the composite material.

Finally the loss of stiffness due to damage on the interface elements leads to the final failure (3). From there on, fully damaged elements will no longer contribute to the connection and the crack will grow as the interface elements will be gradually damaged. The damage evolution is controlled by a scalar variable D which represents the overall damage in the material and evolves from 0 (undamaged) to 1 (fully damaged). The stress components are affected by the damage according to these equations :

$$\begin{cases} \sigma_{zz} = (1-D)\overline{\sigma_{zz}} \text{ if } \overline{\sigma_{zz}} \geq 0 \\ \tau_{xz} = (1-D)\overline{\tau_{xz}} \\ \tau_{yz} = (1-D)\overline{\tau_{yz}} \end{cases} \tag{2}$$

where $\overline{\sigma_{zz}}$, $\overline{\tau_{xz}}$ and $\overline{\tau_{yz}}$ are the stress components predicted by the elastic traction-separation behavior without damage. Two parameters define the damage evolution. The first one is the interfacial strength τ^0. The second parameter that controls the damage evolution is the fracture

toughness G_c. It corresponds with the entire area under the damage law as represented in Figure 2.

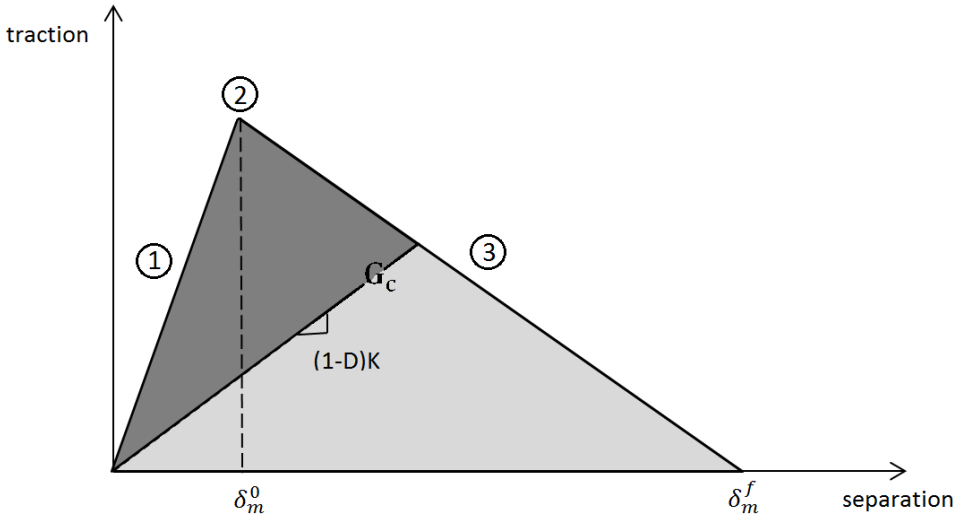

Figure 2. Cohesive law representation.

The damage evolution variable D could be defined by a linear, as shown in Figure 2, or by an exponential softening law for example. On this same figure, δ_m^f corresponds to the effective displacement at complete failure.

3.2. Finite Element Model

The use of the cohesive elements requires specific precautions to be modeled with finite elements. First, it is preferable to model a single interface with cohesive elements to avoid the gradual damage effects on the neighboring layers. This interface is determined experimentally as the delamination location (on the present case, one of the interfaces between $+\theta$ and $-\theta$ plies). By persisting in this approach, the calculation time is reduced and the divergence issues mainly avoided. The first step is to define the initial stiffness of the interface elements. It has been proved that this stiffness K must be around 10^6 N/mm^3 for thicknesses from 0.125 mm to 5 mm [5]. The layers thickness of the T800/M21 layers being 0.175 mm, so this value of K will be used.

A particular attention must be given to the mesh. Indeed, the acceptable mesh size has to be found along the cohesive zone in order to minimize calculation time and also to obtain reliable results. In this aim, it has been shown [5] that the cohesive zone has to be correctly modeled by spatial discretization of finite elements. It happens when the ”process zone”, which is defined as the cohesive zone length where the damage variable D is strictly between 0 and 1, contains more than three elements. This number of elements, represented by the parameter N_e, can be obtained thanks to the formula :

$$N_e = \frac{MEG_c}{l_e(\tau^0)^2} \tag{3}$$

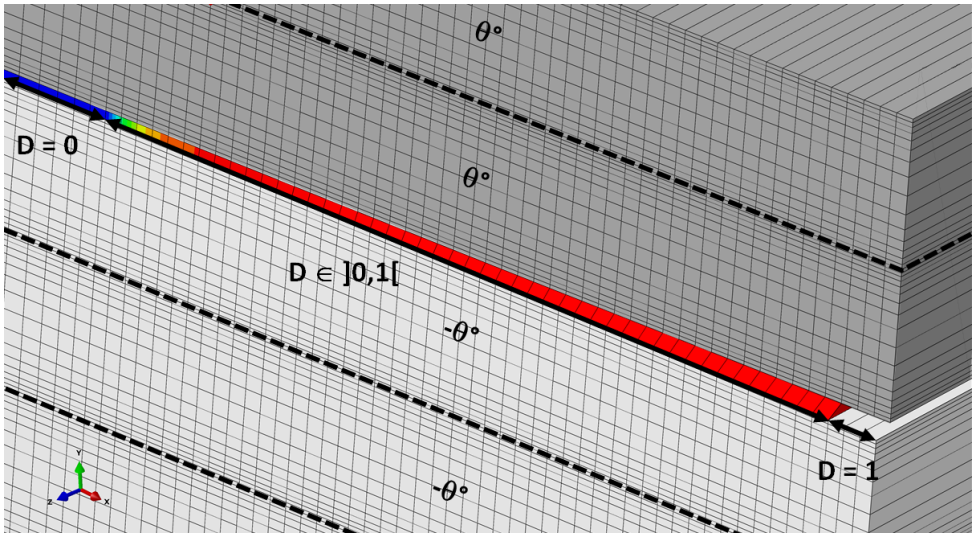

Figure 3. Process zone illustration.

where M is a parameter which depends on each cohesive zone model. In the following study, the value of 0.21 will be chosen, according to the Hui model [6]. E is the transverse Young modulus, G_c is the critical energy release rate, τ^0 is the maximum interfacial strength and l_e is the mesh size in the direction of crack propagation. With the T800/M21 composite material and in compliance with its properties previously seen in Table 1, l_e is found out with N_e = 10, M = 0.21, E = 8 GPa, G_c = 0.74 N/mm and τ^0 = 75 MPa. As a result, mesh size along the interface has to be around 0.02 mm according to equation (3). This mesh size is regular on one millimeter length from the edge. The "process zone" principle and the mesh used can be seen in Figure 3.

To improve calculation time, specific boundary conditions have been specified on the studied composite lay-ups. Indeed, instead of directly applying a load on a side of the entire composite lay-up, the load is applied on an elementary model, with the same width, the same thickness, and a unit length. It is achievable thanks to a Python script which associates the displacements of the nodes of the front side to those of the back side in order to respect the boundary conditions of the full model, as illustrated in Figure 4. It is reflected by these equations :

$$\begin{cases} u_x^{front} = u_x^{back} + \varepsilon x \\ u_y^{front} = u_y^{back} \\ u_z^{front} = u_z^{back} \end{cases} \tag{4}$$

where $\vec{x}$ is the traction direction, $\vec{z}$ is the normal direction and ε the associated strain. The load is applied through a reference point associated to the front face.

4. Results & discussion

As previously discussed, delamination appears through three different steps illustrated in Figure 2 : (1) an elastic part associated with the initial stiffness K, (2) the damage initiation associated

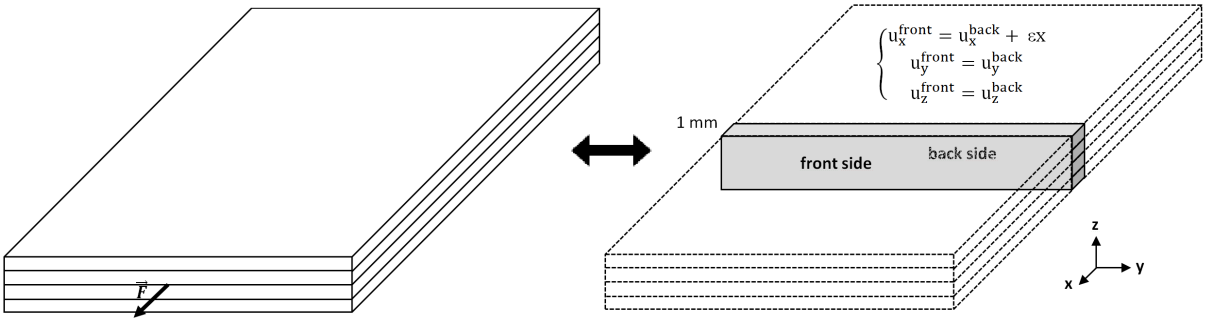

Figure 4. Boundary conditions of the elementary model on a $[\pm\theta]_s$ composite lay-up.

with a damage initiation criterion and (3) the final failure associated with a softening law. These three parameters have been analyzed in order to determine their influence on the damage law.

First, the initial stiffness K does not influence the final failure (Figure 5 (a)). It only changes the damage initiation momentum because the area under the curve still remains the same. In other words, the energy release rate G_c being the same, no matter what initial stiffness is chosen if it is high enough [5]. In the present case, the damage initiation criterion has no impact on the damage momentum. Indeed, the specimens are subjected to quasi-pure mode III [3]. The damage initiation appears when the stress is about 74 MPa, which is the peak value of the nominal stress when the deformation is purely in the first shear direction (Figure 5 (b)). For the same reason (quasi-pure mode III), the choice of the mixed-mode propagation criterion does not matter, including under the Benzeggagh-Kenane [7] form or the power law form. Finally, the exponential or the linear softening law affects the final failure as illustrated in Figure 5 (c). Indeed, the exponential law is "flatter" than the linear one and the energy release rate G_c being the same regardless of the law chosen, the failure jump displacement is higher. As a result, the linear softening law is more conservative than the exponential law.

The failure stresses predicted by the studied cohesive zone models, associated with a linear and an exponential softening law, and those obtained by the experimental campaign presented in [3] are summarized in Table 2. It should be noted that the experimental results are the average values obtained on the five tested specimens for each orientation. The failure stress obtained by the cohesive zone model corresponds to the stress value reaches when the first element of the cohesive zone is fully damaged (D=1).

Lay-up	**Experimental** (MPa)	**Linear** (MPa)	**Exponential** (MPa)	**Diff lin** (%)	**Diff exp** (%)
$[\pm 10_2]_s$	1046	786	828	24.9	20.8
$[\pm 20]_s$	866	789	831	8.9	4.0
$[\pm 20_2]_s$	681	531	560	22.0	17.8
$[\pm 20_3]_s$	586	426	448	27.3	23.6
$[\pm 30_2]_s$	413	391	422	5.3	-2.2

Table 2. Experimental and models results comparison of the failure stresses

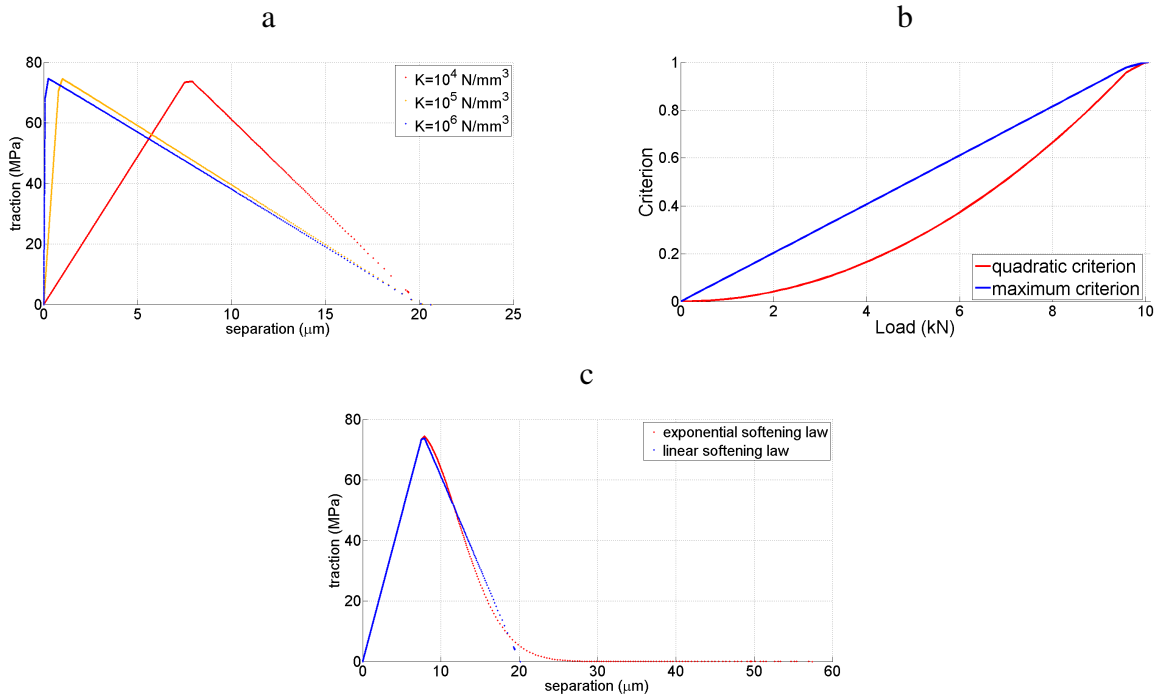

Figure 5. Influence of the cohesive zone model parameters on the $[\pm 20_2]s$ lay-up. (a) Influence of the initial stiffness K, (b) influence of the damage initiation criterion, (c) influence of the softening law.

As previously said, the test specimens can be divided in two distinct groups. The first set (A) is used to evaluate the influence of the plies clustering ($[\pm 20]_s, [\pm 20_2]_s, [\pm 20_3]_s$). The second set (B) considers the influence of the plies orientation ($[\pm 10_2]_s, [\pm 20_2]_s, [\pm 30_2]_s$). The predictions with cohesive elements for the set A show the same tendency that the one observed with the experimental results. In fact, in both cases the failure stress drops with the increase of the composite thickness. The difference between the experimental data and the cohesive elements prediction reaches a maximum value of 27.3% for the $[\pm 20_3]_s$ lay-up with the linear softening law. As for the set B, the more the plies are oriented, the more the failure rupture is low. In this group the maximum difference is observed for the $[\pm 10_2]_s$ orientation and it is of 24.9%. The minimum difference is achieved for the $[\pm 30_2]_s$ lay-up and this minimum value is equal to 2.2% with an exponential softening law. To finish, all the failure stresses predicted by the cohesive zone model associated with a linear softening law are conservative. On the contrary, those used with an exponential softening law are more accurate (an average mistake of 13.7% compare with 17.7% for the linear cohesive zone model), but in one case it is non-conservative.

5. Conclusions

The influence of different cohesive zone models parameters have been compared thanks to an experimental campaign for the prediction of free-edge delamination. For the studied material, only the choice of the softening law has an influence on the displacement jump at failure. Then, the cohesive zone model provides good results compared to those obtained experimentally. Indeed, the difference between the prediction of the cohesive zone model and the average value of the experiments ranges between 2.2% and 27.3%. However, in this study the specimens have a simple geometry and the computational cost can be quickly very heavy for large parts.

Indeed, the use of cohesive elements requires a very fine mesh, which cannot be affordable in some cases, especially in industries. To an experimental point of view, it will be important to propose an specific test to validate in a more accurately way cohesive zone models. Indeed, it could be interesting to propose a test with a mixed-mode ratio and with a progressive failure of the interface.

Acknowledgments

The first author (A. Uguen) acknowledges the financial support of the DGA and of the Brittany region.

References

[1] E. Martin, D. Leguillon, and N. Carrère. A twofold strength and toughness criterion for the onset of free-edge shear delamination in angle-ply laminates. *International Journal of Solids and Structures*, 47:1297–1305, 2010.

[2] A. Turon, P.P. Camanho, J. Costa, and J. Renart. Accurate simulation of delamination growth under mixed-mode loading using cohesive elements: Definition of interlaminar strengths and elastic stiffness. *Composite Structures*, 92:1857–1864, 2010.

[3] L. Zubillaga, N. Carrère, A. Turon, and G. Guillamet. Experimental and numerical analysis of free-edge delamination by means of a two-fold criterion and a cohesive zone model. *Composites Part A*, submitted.

[4] Abaqus documentation, Version 6.12. Simulia, 2012.

[5] A. Turon, C.G. Dávila, P.P. Camanho, and J. Costa. An engineering solution for mesh size effects in the simulation of delamiation using cohesive zone models. *Engineering Fracture Mechanics*, 74:1665–1682, 2007.

[6] C.Y. Hui, A. Jagota, S.J. Bennison, and J.D. Londono. Crack blunting and the strength of soft elastic solid. *Proceedings of the Royal Society of London A*, 459:1489–1516, 2003.

[7] M.L. Benzeggagh and M. Kenane. Measurement of mixed-mode delammination fracture toughness of unidirectional glass/epoxy composites with mixed-mode bending appartus. *Composite Science and Technology*, 56:439–449, 1996.